

1 **Air-interfaced colonization model suggests a commensal-like interaction of**
2 ***Neisseria meningitidis* with the epithelium, which benefit from colonization**
3 **by *Streptococcus mitis*.**

4
5 **Mathilde Audry^{1,2,3}, Catherine Robbe-Masselot⁴, Jean-Philippe Barnier^{1,2,3,7}, Benoit**
6 **Gachet^{1,2,3}, Bruno Saubaméa⁵, Alain Schmitt^{2,6}, Sophia Schönherr-Hellec^{1,2,3}, Renaud**
7 **Léonard⁴, Xavier Nassif^{1,2,3,7} and Mathieu Coureuil^{1,2,3,*}**

8
9 ¹ Inserm, unité U1151, Institut-Necker-Enfants-Malades, Paris, Paris, France

10 ² Université de Paris, Faculté de médecine, Paris, France.

11 ³ CNRS, UMR 8253, Paris, France

12 ⁴ Univ. Lille, CNRS, UMR8576-UGSF-Unité de Glycobiologie Structurale et Fonctionnelle,
13 Lille, France

14 ⁵ Cellular and Molecular Imaging facility, Inserm US25, UMS3612 CNRS, Faculté de
15 Pharmacie de Paris, Université de Paris, Paris, France

16 ⁶ Institut Cochin, Inserm U1016, Paris, France

17 ⁷ Assistance Publique – Hôpitaux de Paris, Hôpital Necker Enfants Malades, Paris, France

18

19 * Corresponding authors: mathieu.coureuil@inserm.fr

20

21

22

23

24

25

26 **ABSTRACT**

27 *Neisseria meningitidis* is an inhabitant of the nasopharynx, from which it is transmitted from
28 person to person or disseminates in the blood and becomes a harmful pathogen. In this work,
29 we addressed the colonization of the nasopharyngeal niche by focusing on the interplay
30 between meningococci and the mucus that lines the mucosa of the host. Using Calu-3 cells
31 grown in air-interfaces culture, we studied the meningococcal colonization of the mucus and
32 the host response. Our results suggested that *N. meningitidis* behaved like commensal bacteria
33 in mucus, without interacting with human cells or actively transmigrating through the cell
34 layer. As such, meningococci did not trigger a strong innate immune response from the Calu-
35 3 cells. Finally, we have shown that this model is suitable for studying interaction of *N.*
36 *meningitidis* with other bacteria living in the nasopharynx, and that *Streptococcus mitis* but
37 not *Moraxella catarrhalis* can promote meningococcal growth in this model.

38

39

40

41

42

43

44

45

46

47

48

49

50

51

52 INTRODUCTION

53 *Neisseria meningitidis* (the meningococcus) is a Gram-negative bacterium that
54 normally resides asymptotically in the human nasopharynx. For unknown reasons it may
55 cross the epithelial barrier and proliferate in the bloodstream where it becomes one of the
56 most harmful pathogens. *N. meningitidis* effectively adheres to the endothelial cells lining the
57 lumen of blood vessels¹. From there, bacteria proliferate and cause blood vessel dysfunction
58²⁻⁶ responsible for the rapid progression of septic shock, leading in the worst case to *purpura*
59 *fulminans*, an acute systemic inflammatory response associated with intravascular coagulation
60 and tissue necrosis. *N. meningitidis* can also cross the blood-brain barrier and cause
61 cerebrospinal meningitis^{7,8}.

62 *N. meningitidis* is transmitted from person to person by aerosol droplets produced by
63 breathing, talking, coughing or by direct contact with a contaminated fluid. The natural
64 reservoir of *N. meningitidis* is the human nasopharynx mucosa, located at the back of the nose
65 and above the oropharynx. There, the bacteria encounters a rich microbiota⁹⁻¹¹ that
66 continuously undergoes changes with age and upon upper respiratory infections^{12,13}. The
67 nasopharynx is lined with two main types of epithelium: a pluristratified squamous epithelium
68 that covers 60% of the nasopharynx and a columnar respiratory epithelium^{14,15}. In the
69 respiratory tract, cells are protected by a 10-12 μm thick two-layer surface liquid formed by a
70 low-viscosity periciliary liquid (PCL) in contact with the cells and a high-viscosity mucus
71 facing the lumen that retains bacteria, inhaled particles and cell debris (outer mucus)^{16,17}. The
72 PCL facilitates ciliary beating that allows effective mucociliary clearance at 6.9 ± 0.7 mm/min
73¹⁸. By constantly transporting mucus from the lower respiratory tract to the pharynx from
74 where it is swallowed, this mechanism is considered as the main defense against
75 microorganisms and particles. The mucus layer in which commensal bacteria are restricted is
76 a thick gel formed by mucins and contains many antimicrobial proteins and peptides such as

77 IgA, lysozyme, lactoferrin and human defensins¹⁹⁻²¹. Mucins are a family of at least 22 high
78 molecular weight glycoproteins divided into two classes: membrane associated mucins that
79 are produced by any epithelial cell and gel-forming mucins produced by goblet cells and
80 submucosal glands. In the respiratory tract, the mucus layer is mainly composed of MUC5AC
81 and MUC5B. Their expression is tightly regulated and responds to bacterial infections and to
82 a variety of respiratory tract diseases¹⁷.

83 The interaction of *N. meningitidis* with epithelial cells has been the subject of
84 numerous studies over the past four decades. However, the means by which meningococci
85 cross the nasopharyngeal wall is still under debate. This may be due to the lack of convenient
86 and relevant model mimicking the nasopharyngeal niche. Most of the previous studies,
87 addressing the adhesion-dependent interaction of *N. meningitidis* with intestinal and
88 respiratory tract epithelial cells, have been performed on cells cultured in liquid media such as
89 RPMI and DMEM. These first studies gave rise to the concept of type IV pili- and/or
90 Opa/Opc-mediated cell colonization. In such a model, meningococci interact with epithelial
91 cells through their type IV pili and form highly proliferative microcolonies that eventually
92 cross the epithelial barrier²²⁻²⁸ while Opa and Opc proteins are involved in an active
93 internalization process that is supposed to promote the translocation of bacteria through the
94 cell monolayer²⁹⁻³¹. Each of these works demonstrated a close interaction of *N. meningitidis*
95 with human epithelial cells. Over the last decade, few studies have focused on the
96 translocation of *N. meningitidis* through the epithelial wall. The work of TC Sutherland in
97 2010³² addresses this question by using Calu-3 human bronchial epithelial cells, a respiratory
98 tract cellular model that can be fully differentiated into a polarized epithelium. Although the
99 authors worked with cells infected in liquid-covered culture (LCC), they proposed to use
100 Calu-3 cells in air-interfaced culture (AIC), a model in which the cells are grown with the
101 apical domain facing the air. They finally concluded that *N. meningitidis* may cross the

102 epithelial layer by the transcellular route using type IV pili. Meanwhile, Barrile *et al* have
103 shown, using Calu-3 cells cultured in LCC, that meningococci may be internalized and
104 transported to the basal domain by subverting the intracellular traffic of the host cells ³³.
105 However, they have also shown that the translocation of bacteria was fully inhibited in highly
106 polarized cells cultured for 18 days.

107 In addition to these works, a series of *ex vivo* experiments were carried out between
108 1980 and 1995 using organ cultures instead of immortalized cells ³⁴⁻³⁷. The authors have
109 observed a direct interaction between meningococci and explant epithelial cells. This has been
110 associated with the loss of cilia and, for some explants, with the internalization of bacteria in
111 epithelial cells. However, in each of these experiments, the explants were immersed in liquid
112 medium, a protocol that may have altered cell morphology and disrupted the mucus barrier.

113

114 The study of meningococcal colonization of the human upper respiratory tract has
115 been hampered by the lack of relevant models. In this work, we took advantage of Calu-3
116 cells grown under AIC ³⁸ to study how meningococci colonize the nasopharyngeal niche.
117 Infection of Calu-3 cells revealed the dependence of *N. meningitidis* on mucus in this model.
118 Our results suggest that the mucus protects meningococci against death associated with
119 desiccation and support growth of bacteria. We have shown that the mucus layer sequestered
120 bacteria and that a firm interaction of bacteria with the epithelial cells was rarely observed.
121 Bacteria grew without triggering a strong innate immune response from the Calu-3 cells.
122 Embedded in the mucus, meningococci were protected and fed, expressed less adhesion
123 factors, a high level of iron transporters and type IV pili were not necessary for colonization.
124 Finally, we evaluated the effect of *Streptococcus mitis* and *Moraxella catarrhalis*
125 colonization, two bacteria classically present in the nasopharynx mucosa, on the growth of *N.*
126 *meningitidis* ³⁹⁻⁴¹ and showed that co-colonization of *N. meningitidis* with *S. mitis* can

127 promote meningococci growth.

128

129

130

131

132

133

134

135

136

137

138

139

140

141

142

143

144

145

146

147

148

149

150

151

152 **RESULTS**

153 **Meningococci require mucus production to colonize cells cultured in air-liquid interface.**

154 To study the colonization of the human upper respiratory tract by *N. meningitidis*, we used
155 Calu-3 cells cultured on 0.4 μ m pore membrane under AIC. Cells maintained for a few days in
156 AIC (Week 0) formed a mono-stratified epithelium with only a few spots of mucus on the cell
157 surface (**Figure S1A**). After two weeks of AIC, we observed pseudo-stratified Calu-3 cells
158 covered with a mucus layer. After three weeks under AIC, the epithelium appeared pluri-
159 stratified with a thick layer of mucus above the cells (**Figure S1A**). Cells cultured for 2 weeks
160 under AIC also revealed the presence of tight junction, microvilli and mucus producing cells
161 (**Figure S1B**). We first considered whether mucus may influence the growth of meningococci
162 on Calu-3 cells cultured under AIC for two days or two weeks (AIC W₀ and AIC W₂,
163 respectively). We added 1.10⁶ meningococci (strain 2C4.3) on the top of cells and assessed
164 epithelial colonization by confocal imaging and quantitative culture (CFU counts), 24 hours
165 after infection. These results were compared to those obtained after infection of Calu-3 cells
166 cultured under liquid-covered culture (LCC). We observed a dramatic decrease in bacterial
167 proliferation 24 hours after infection of AIC W₀ cultured cells compared to LCC cultured
168 cells (1.35x10⁸ +/- 0.35x10⁸ bacteria per well in LCC; 0.75x10⁶ +/- 0.25x10⁶ bacteria per well
169 in AIC W₀). This inhibition is less pronounced in AIC W₂ cultured cells that produced mucus
170 (2x10⁷ +/- 0.64x10⁷ bacteria in AIC W₂) (**Figure 1A and 1B**). This result suggests that AIC
171 infection is more challenging for meningococci than LCC infection and that the presence of
172 mucus partially compensates for this defect.

173

174 The mucus layer is known to be a poor nutritive medium that limits the growth of many
175 commensal and pathogenic bacteria. It is a highly hydrated gel that also protects the cell
176 surface from desiccation. We therefore aimed at determining whether the mucus layer could

177 protect *N. meningitidis* against desiccation in an abiotic surface colonization model (**Figure**
178 **1C**). We infected plastic wells coated with purified mucus and applied desiccation condition
179 to meningococci for 30, 60 and 120 minutes. Meningococci were particularly sensitive to
180 desiccation. In the uncoated wells (without mucus), the number of living bacteria was reduced
181 by 5.6×10^3 fold at 30 minutes and 7.9×10^5 fold at 120 minutes after the beginning of the
182 experiment. Conversely, in mucus-covered wells, the number of living bacteria was reduced
183 by 0.11×10^3 fold at 30 minutes and 1.46×10^3 fold at 120 minutes after the beginning of the
184 experiment. Overall, our results indicate that the mucus layer of Calu-3 cells cultured in AIC
185 protect bacteria from desiccation.

186

187 **Meningococci are restricted in the mucus layer and do not cross the epithelium.**

188 During LCC infection, bacteria readily adhere to human cells and induce host-cell signaling
189 leading to the recruitment of ezrin and actin and the formation of membrane protrusions^{42,43}.
190 Conversely, during AIC infection, as it would be the case during colonization of
191 nasopharyngeal mucus, bacteria are deposited on the mucus layer that protects the cells. We
192 therefore studied how *N. meningitidis* interact with the epithelium cultured under AIC. First,
193 we compared the number of CFU recovered from the outer mucus with a fraction containing
194 cells and the cell-attached mucus. The cells were infected with 10^6 wild type meningococci or
195 its non-piliated derivative (*pile* mutant; $\Delta pile$), which is unable to adhere to human cells²⁴.
196 Up to 80% of wild-type or $\Delta pile$ meningococci have been recovered in the outer layer of the
197 mucus, which means that *N. meningitidis* only penetrate slightly through this layer (**Figure**
198 **2A**). Interestingly, the same amount of wild-type and $\Delta pile$ meningococci was collected in the
199 fraction containing cells and the cell-attached mucus. To better characterize the infection of
200 Calu-3 cells grown using AIC, and determine if the bacteria interacted with the cells, we
201 visualized infected cells by transmission and scanning electron microscopy (TEM and SEM).

202 We found that most bacteria were trapped in the mucus (**Figure 2B**), and organized into small
203 aggregates of living and dying meningococci, according to cell morphology. Only few
204 bacteria were found in direct contact with Calu-3 cells plasma membrane and we did rarely
205 detect membrane protrusions near bacteria, in contrast to what has been observed previously
206 when cells were infected in LCC⁴³. We detected only few internalized bacteria, despite
207 analysis of four different longitudinally cut cell layers. These bacteria were in the vicinity of
208 the apical plasma membrane (**Figure 2D**) or already digested in a vacuole (**Figure S2**). We
209 then studied the infected Calu-3 cells by confocal microscopy. Again, most bacteria were
210 detected in the mucus, stained with anti-MUC5AC antibody. We also observed both by
211 confocal microscopy and TEM, microcolonies of bacteria trapped between epithelial cells in
212 cavities in the upper part of the cell layer (**Figure 3A, B**). However, no bacteria were
213 observed at the basal part of the epithelium as would have been expected if the bacteria had
214 passed through it. In addition, non-piliated $\Delta pilE$ mutant showed the same spatial location as
215 the wild type strain, suggesting that type IV pili have no role on the location of bacteria in the
216 mucus (**Figure 3A**).

217 Based on this observation, we studied the translocation of meningococci through the epithelial
218 cell layer. We first grew Calu-3 cells under AIC using 3 μm pore membranes instead of
219 0.4 μm pore membranes. We choose to infect Calu-3 cells with 10^2 or 10^4 bacteria and we
220 first confirmed the proliferation of *N. meningitidis* in these conditions (**Figure S3B, C**).
221 Regardless of the inoculum, the number of colonizing bacteria at 24hrs, 10^7 CFU, was similar.
222 We then studied the translocation of *N. meningitidis* from the mucus to the basal chamber, by
223 plating the basal media on agar plates, at 4 and 24 hours after infection. We considered a
224 positive translocation when at least one CFU has been recovered from the basal chamber.
225 Interestingly, 24 hours after infection, we detected only 2 out of 16 colonized basal chambers
226 in total, and no bacteria were recovered in the basal chambers 4 hours after infection (**Figure**

227 **3C**). Using this model, we then evaluated the effect of IL-4 or IL-13, two cytokines known to
228 be involved in pharyngeal inflammation ⁴⁴, on the translocation of *N. meningitidis*. The cells
229 were treated 24 hours with 5 ng/ml IL-4 or IL-13 as previously described ⁴⁴ (**Figure 3C**). As
230 expected, the treatment of Calu-3 cells with IL-4 or IL-13 resulted in a 2-fold decrease in
231 TEER (165.9±20.02 Ω.cm² and 155.3±11.58 Ω.cm², respectively; **Figure S2A**). However,
232 this has not been associated with an increased traversal of the cell layer by *N. meningitidis*
233 (**Figure 3C**). Our results indicate that meningococci are likely to colonize the outer layer of
234 mucus, from which bacteria can reach the cell-attached mucus but rarely come into contact
235 with cells or cross the epithelial layer cultured in AIC.

236

237 **Expression of meningococcal virulence factors during air-liquid infection.**

238 Our results suggest that, on mucosa, meningococci are likely to live trapped in the mucus. In
239 these conditions, it is likely that meningococci regulate the expression of their genes
240 differently than in broth. We therefore characterized the relative expression of genes known to
241 be involved in mucosal colonization. We have focused on the expression of genes encoding
242 adhesion factors: *pilE*, *opaB*, *opaC* and *nhbA*; genes encoding proteins involved in iron
243 acquisition: *tbpA*, *lbpA*, *fetA*, and *tonB*; *mtrC* encoding the first gene of the *mtrCDE* operon
244 that is involved in drug efflux; *ctrA* that codes for the capsular transport protein A; and the
245 four genes coding for targets of the MenB vaccine, *porA*, *fhbp*, *nadA* and *nhbA*. We compared
246 the expression of these genes during AIC infection to their expression during the exponential
247 and stationary phase of growth in broth (**Figure 4**).

248 These genes followed different expression profiles. Expression of the adhesion factors (*pilE*,
249 *opaB*, *opaC* and *nhbA*) were comparable between the stationary phase of growth in broth and
250 the infection of Calu-3 cells for 24 hours. In contrast, expression of *pilE*, *opaB*, *opaC* and
251 *nhbA* in AIC was decreased with respect to the exponential phase of growth (AIC/exponential

252 phase: 0.28, 0.34, 0.33 and 0.47 fold, respectively). The three iron transporters tested (*tbpA*,
253 *lbpA*, *fetA*) were strongly expressed in AIC compared to the exponential phase of growth
254 (AIC/exponential phase: 6.25, 10 and 27 fold, respectively).

255 It is noteworthy that *fhbp*, *tonB*, *mtrC* expression were weak during AIC infection. Their
256 expressions were 6.3, 6.7 and 3.5 fold less expressed in the mucus of Calu-3 cells than in the
257 stationary phase of growth. No major difference in the expression of *nadA*, *porA* and *ctrA* was
258 observed between the tested conditions. Overall, nine out of the thirteen tested genes appeared
259 to follow the same pattern of expression in AIC than in the stationary phase of growth.

260

261 **Meningococci trigger less inflammation in AIC condition**

262 We then addressed the impact of meningococcal colonization on the innate immune response
263 of Calu-3 cells grown in AIC or LCC. We therefore measured the release of ten pro- or anti-
264 inflammatory cytokines 24 hours after infection in comparison to the basal release of these
265 cytokines by Calu-3 cells after 24 hours of culture without bacteria (**Figure 5**). After infection
266 we observed that three cytokines were produced in higher amount under LCC infection than
267 AIC infection: IL1 β : 2.9 fold increase under AIC versus 15.6 fold increase under LCC;
268 TNF α : 66.4 fold increase under AIC versus 200.4 fold increase under LCC; IL-4: 6 fold
269 increase under AIC versus 31.8 fold increase under LCC. A moderate release of four other
270 cytokines was only detected under LCC: IL-10, IL-13, IL-2 and IL-6 (1.4 fold increase, 1.5
271 fold increase, 1.6 fold increase and 2.33 fold increase, respectively). Finally, IFN γ secretion
272 was increased by 2 fold under AIC versus 3 fold under LCC, and IL-12 secretion was
273 increased by 3.1 fold under AIC versus 5.1 fold under LCC. Altogether, the pro-inflammatory
274 response assessed by cytokine production, appeared to be higher in the LCC model compared
275 to the AIC model. In addition, during an AIC infection we did not observe any secretion of
276 IL-2, IL-10, IL-13 and IL-6.

277

278 ***Streptococcus mitis* colonization of Calu-3 cells promotes *Neisseria meningitidis* growth.**

279 We next aimed at studying in this model the interplay between *N. meningitidis* and other
280 bacterial species. Among species known to colonize the human nasopharynx, we selected *S.*
281 *mitis* and *M. catarrhalis* as representative bacteria³⁹⁻⁴¹. We first infected Calu-3 cells,
282 cultured in AIC on a 0.4µm pore membrane, with 1.10^5 *S. mitis* or *M. catarrhalis*. Both were
283 able to survive in the mucus of Calu-3 cells, but we did not detect proliferation 48 hours after
284 infection (*S. mitis*, inoculum: $3.08 \times 10^5 \pm 0.8 \times 10^5$, 48 hours: $2.7 \times 10^5 \pm 1.01$; *M. catarrhalis*,
285 inoculum: $4.12 \times 10^5 \pm 1.9 \times 10^5$, 48 hours: $6.07 \times 10^5 \pm 2.38$). We then infected Calu-3 cells
286 colonized by *S. mitis* or *M. catarrhalis* with 1×10^6 meningococci (wild-type 2C4.3 strain) for
287 24 hours (**Figure 6**). As control, naïve uninfected Calu-3 cells were infected by *N.*
288 *meningitidis*. Our results showed that the co-infection with *S. mitis* significantly improved
289 meningococcal colonization while *M. catarrhalis* had no effect (**Figure 6**). Interestingly, the
290 positive effect of the *S. mitis/N. meningitidis* co-infection on the growth of meningococci
291 appeared to be specific of the AIC model. A 24 hours broth co-culture of 1.10^5 *S. mitis* and
292 1.10^6 *N. meningitidis* revealed a slight decreased in meningococcal growth (**Figure S4A**).
293 Overall, these results support the hypothesis that *N. meningitidis* growth in AIC may be
294 facilitated by other bacteria of the nasopharyngeal niche.

295 Unlike *M. catarrhalis*, *S. mitis* is able to hydrolyze glycans, which are very abundant on
296 mucin proteins⁴⁵. The hydrolysis of mucins' carbohydrates might thus provide an additional
297 source of carbon and nutrient for meningococci, which could be responsible for a significant
298 increase in meningococcal colonization. We investigated mucins' glycosylation profiles by
299 mass spectrometry after infection or co-infection of Calu-3 cells with *S. mitis* and *N.*
300 *meningitidis* (**Table 1 and S1**). We observed a moderate sialylation of mucins after
301 meningococcal colonization, since 59% of the oligosaccharides detected were sialylated

302 compared to 36.2% in non-infected cells. The glycosylation profile of mucins has changed
303 dramatically after infection with *S. mitis* (**Table 1 and S1**). We noticed a complete release of
304 sialic acid from the mucins and a global simplification of the O-glycans, while infection with
305 inactivated streptococci did not alter the glycosylation profile of mucins (**Table S1**). This
306 confirms that *S. mitis* is capable of hydrolyzing mucins' O-glycans. A process that correlates
307 with an increased growth of *N. meningitidis*.

308

309

310

311

312

313

314

315

316

317

318

319

320

321

322

323

324

325

326

327 **DISCUSSION**

328 In this work, we adapted an experimental model, based on Calu-3 cells cultured in AIC, to
329 study the behavior of *N. meningitidis* in the mucus of the respiratory tract. We have shown
330 that meningococci are trapped in the mucus layer where bacteria are protected from
331 desiccation and are likely to find nutrients to grow. We found no evidence of an active
332 passage of *N. meningitidis* through the epithelial layer and we observed that type IV pili were
333 not important for growth or motility/mobility in this model. Similarly, we showed that
334 virulence factors were poorly expressed in this model compared to culture in broth. Strikingly,
335 this suggests commensal-like behavior of *N. meningitidis*, a hypothesis that is supported by
336 the poor cytokine response observed 24 hours after infection. We took advantage of this
337 model to investigate the effect of other bacteria on the growth of *N. meningitidis*. We have
338 shown that *S. mitis*, which is able to hydrolyze glycans, facilitates the growth of meningococci
339 in a co-infection protocol.

340

341 Most studies aimed at determining the behavior of meningococci on epithelial cells has been
342 done with cells that have been cultured and infected in LCC. Although these investigations
343 provided a comprehensive description of the interaction between *N. meningitidis* and human
344 epithelial cells, the scientific community has not been able to conclude on the question of how
345 and when meningococci cross the nasopharyngeal epithelium. During LCC infections,
346 bacteria easily proliferate in the cell culture medium that contains amino acids, carbon source
347 and protein extracts. This allows *N. meningitidis* to grow and eventually cover almost
348 completely the Calu-3 cell layer. When we infected Calu-3 cells cultured in AIC for 2 weeks,
349 we observed a 6 fold decrease in the total number of CFU per filter 24 hours after infection.
350 The bacteria were mainly found in the mucus where they organized into small groups of
351 living and dying meningococci. As a consequence, bacteria rarely interact with human cells

352 and we have barely found *N. meningitidis* in direct contact with the plasma membrane of
353 these cells. In view of this result, we asked if *N. meningitidis* can cross the epithelial layer
354 grew in AIC. After infection of cells cultured on 3 μm pore membranes, we detected bacteria
355 in the basal chamber of only 2 out of 8 wells for the highest inoculum (10^4 CFU) and 0
356 contaminated chambers for the lowest (10^2 CFU). We then treated Calu-3 cells with IL-4 or
357 IL-13 for 24 hours, two cytokines that induce TEER decrease and induce mucus production
358 ⁴⁴. As expected, these two cytokines led to a reduction in TEER. But, this has not been
359 followed by an increase in the translocation of bacteria through the epithelial layer. All these
360 results suggested that the traversal observed in this experiment was only stochastic and
361 probably due to the heterogeneity of the mucus layer on the surface of the wells. To support
362 this hypothesis, we have never observed any bacteria, inside or outside the cells, and in the
363 vicinity of the porous membrane.

364

365 These results suggest that *N. meningitidis* growing in the mucus of epithelial cells did not alter
366 the epithelial layer during the course of the experiment. We therefore studied the production
367 of cytokines by epithelial cells grown in AIC or in LLC. Strikingly, we observed that three
368 major inflammatory cytokines (IL-6, TNF α and IL-1 β) were produced less during infection in
369 AIC than in LCC. The two anti-inflammatory cytokine IL-10 and IL-4 were also produced
370 less after infection, suggesting an overall reduction in the cytokine response during infection
371 in AIC. However, after infection, Calu-3 cells secreted IL-12 and IFN γ to the same extend
372 whether infection was in AIC or LCC. IFN γ and IL-12 are known to be associated with
373 macrophage and dendritic cells response, although there are evidences that epithelial cells
374 produce these cytokines after infection with microbes ^{46,47}. IFN γ has pleiotropic effects on the
375 epithelial cells of the respiratory tract. This cytokine has been shown to reduce MUC5AC
376 expression, which may lead to a decrease in the barrier property of the respiratory mucus ⁴⁸.

377 In the meantime IFN γ induces the expression of CEACAM receptors⁴⁹ that are the receptors
378 for the meningococcal adhesin Opa, known to be involved in the internalization of bacteria.
379 Conversely, IFN γ may promote the barrier function of lung epithelial cells⁴⁴. Finally, we did
380 not detect IL-8 secretion after infection of Calu-3 cells. In our cytokine assay, AIC cultured
381 cells were generally less reactive than cells that have been cultured in LCC, indicating that the
382 mucus layer is likely to protect cells and retain pathogen-associated molecular patterns,
383 resulting in a reduction in the innate immune response. However, our model, which did not
384 include immune cells, only gave a partial overview of the innate immune response.

385

386 We observed that the expression of virulence factors by *N. meningitidis* varied accordingly to
387 growth status and that three virulence genes *pilE*, *mtrC* and *fHbp* were significantly silenced
388 during infection in AIC. The expression of *pilE* during infection of the AIC model appeared
389 to be similar to that observed during the stationary phase of growth in liquid culture. This was
390 correlated with the absence of a role for type IV pili during the colonization of Calu-3 cells.
391 Although most of the meningococcal strains found *in vivo* were piliated, the role of type IV
392 pili during growth in the mucus was probably not related to motility and/or interaction with
393 epithelial cells. However, we could not exclude an interaction between type IV pili and
394 mucins. Conversely, the expression of *fHbp* during infection in AIC was dramatically
395 decreased compared to the exponential and stationary phase of growth in broth. This suggests
396 that mucus is sensed by bacteria and in which *N. meningitidis* will adapt the expression of its
397 virulence genes. Interestingly, fHBP is a key virulence factor of *N. meningitidis*⁵⁰ necessary
398 for binding to human factor H and that inhibits the host alternative complement pathway. The
399 role of fHBP in the respiratory tracts is not clear. While the respiratory mucus contains
400 complement components^{51,52}, the bactericidal activity itself of the complement is not clearly
401 defined against *N. meningitidis*. For instance, acapsulated strains are regularly recovered by

402 swabbing whereas an active component system should have eliminated these strains. It was
403 therefore not surprising to observe the lack of regulation of *ctrA* gene expression between the
404 different conditions tested. Based on our results, and in the context of the MenB vaccine, it
405 may be important to further investigate the expression of *fHbp* in the context of respiratory
406 mucus. Finally we showed that *lbpA*, *tbpA* and *FetA* were highly expressed in AIC,
407 confirming the low concentration of free iron in this model.

408

409 The nasopharynx is colonized by six main genera: *Haemophilus*, *Streptococcus*, *Moraxella*,
410 *Staphylococcus*, *Alloiococcus* and *Corynebacterium*^{40,41}. The impact of the microbiota on the
411 growth, survival and expression of *N. meningitidis* virulence factor is not yet known. Here, we
412 have used the AIC model to address the impact, on *N. meningitidis* growth, of the
413 colonization by two of these bacteria. We infected Calu-3 cells with *S. mitis* or *M. catarrhalis*.
414 Interestingly, we observed that *S. mitis* promoted meningococcal growth 24 hours after
415 infection. This result was not expected since it is known that the pyruvate oxidase (SpxB) of
416 *Streptococcaceae* produces a high amount of hydrogen peroxide and inhibits the growth of *N.*
417 *meningitidis* in broth⁵³. Okahashi has shown that *S. mitis* also expresses SpxB, which may be
418 deleterious for Calu-3 cells⁵⁴. We therefore studied the growth of co-cultured meningococci
419 with *S. mitis* in broth (Figure S4). As described, a high ratio of *S. mitis* killed meningococci,
420 while a ratio of 1 *S. mitis* per 10 *N. meningitidis* is sufficient to reduce the total number of
421 meningococci by two after one day of co-culture. Conversely, in AIC, *S. mitis* promotes the
422 growth of *N. meningitidis*, suggesting that *S. mitis* was less active against meningococci in
423 AIC conditions. In addition, our glycomic analysis indicated that *S. mitis* is capable of
424 hydrolyzing mucin O-glycans while *N. meningitidis* cannot. This was expected since *S. mitis*
425 is known to express many glycosyl hydrolases⁴⁵. Since sialic acids were released from the O-
426 glycans, we assessed whether this could provide a growth advantage for *N. meningitidis*. As

427 anticipated, meningococci were unable to grow in the presence of sialic acid as sole carbon
428 source in broth, and the addition of sialic acid in the mucus of Calu-3 cells was not sufficient
429 to enhance the growth of meningococci (data not shown). However, it can be hypothesized
430 that *S. mitis* might increase the concentration of other nutrients that may be metabolized by *N.*
431 *meningitidis*.

432

433 All together, our results have shown that infection of mucus-producing cells in AIC is
434 different from that of conventional experiments performed in LCC. While these latter works
435 have investigated the interaction of *N. meningitidis* with epithelial cells, which is likely to
436 occur after substantial inflammation or mechanical breach in the mucus layer, our present
437 study emphasizes that *N. meningitidis* is certainly trapped in the mucus layer and rarely
438 interacts with human cells while the host response is less pronounced. Further work will be
439 needed to better understand how *N. meningitidis* regulates its virulence factors and cohabit
440 with other bacterial species in the mucus.

441

442

443

444

445

446

447

448

449

450

451

452 **MATERIALS AND METHODS**

453

454 **Bacterial strains and growth conditions**

455 *N. meningitidis* NEM 8013 (2C4.3), a piliated capsulated serogroup C strain, and its isogenic
456 non-adhesive Pile defective mutant ($\Delta pilE$) were used in this study²⁷.

457 *Streptococcus mitis* B26E10 (referenced as 0902 230473 in Necker Hospital collection) and
458 *Moraxella catarrhalis* B18F4 strains (respectively referenced as B18F4 in Necker Hospital
459 collection) were isolated from a patient in the Necker hospital (Paris). Except for
460 *Streptococcus mitis* strain grown on chocolate agar polyvitex plates, all strains were grown on
461 BHI-agar plates supplemented with 5% horse serum at 37°C in a 5% CO₂ incubator.
462 Antibiotics were used at the following concentrations: kanamycin at 100 µg/ml, vancomycin
463 at 20 µg/ml, polymyxin at 15 µg/ml.

464

465 **Cell culture**

466 Calu-3 epithelial cells (ATCC HTB-55) were maintained in optiMEM medium (Life
467 Technologies) supplemented with 5% fetal bovine serum, HEPES, minimum amino acids
468 solution and penicillin-streptomycin antibiotics. Cells were grown in a 5% CO₂ incubator at
469 37°C. Cells were grown on polyester 0.4 µm pore membrane cell culture filter (Corning,
470 Transwell®). For traversal assays, 3 µm pore membrane were used. Prior to cell seeding,
471 filter's membranes were coated with type IV human placenta collagen (Sigma) for 24 hours.
472 Cells ($3 \cdot 10^5$) were seeded onto the apical side of membranes and were maintained in 200 µl of
473 culture medium in the apical chamber and 1.2 ml in the basal chamber. In AIC conditions, the
474 apical culture media was removed after five days and cells were allowed to grow at air-
475 interface for 3 to 6 days (week 0) or for 14 to 17 days (week 2). Liquid-covered layers were
476 seeded and cultured as described above, except that the apical media were maintained all

477 along. The transepithelial electrical resistance across air interfaced culture was measured with
478 a Millicell[®] Voltohmmeter (Millipore). Notably, the barrier function of the Calu-3 cell layer
479 that have been grown on a 3 μm pore membrane were decreased, as indicated by
480 measurement of the transepithelial electrical resistance (TEER: $357\pm 19.83 \text{ }\Omega/\text{cm}^2$ using 0.4
481 μm pore membrane; $258\pm 14.63 \text{ }\Omega/\text{cm}^2$ using 3 μm pore membrane) (**Figure S3A**).

482

483 **Infection**

484 *Infection with N. meningitidis.* Two days before infection, antibiotics were removed from the
485 culture media. On the day of infection, a suspension of bacteria from an overnight culture on
486 agar plate was diluted to a bacterial concentration of 5.10^7 CFU/ml and cultured for 2 hours at
487 37°C in optiMEM medium. The air-interfaced culture cells were infected on the apical side
488 with a 10 μl of a bacterial suspension containing 10^6 CFU per 10 μl unless specified. The next
489 day, cells were collected by scratching and thoroughly vortexed, then CFU were counted by
490 plating serial dilutions onto agar plates. The same protocol was applied for liquid interface
491 infections, except that a volume of 200 μl of bacterial suspension was used (10^6 CFU per 200
492 μl). In order to separate bacteria present in the outer mucus fraction or in cell-attached mucus
493 fraction, an optiMEM-0.1% N-acetylcysteine solution was incubated for 15 minutes on top of
494 the cells and harvested. This process was repeated 3 times and CFU were counted in this outer
495 mucus fraction by plating serial dilutions. Then for cell-attached mucus fraction, scratching
496 collected cells were vortexed and bacterial loads were assessed by plating CFU.

497 *Transmigration assay.* One day prior infection with bacteria, human interleukine-4 (IL-4) and
498 interleukine-13 (IL-13) were added in the basal chamber of Calu-3 cells cultured in AIC at
499 5 ng/ml each. Media were replaced immediately before infection and IL-4 or IL-13 were
500 added freshly. At 4 and 24 hours post-infection, media from the basal chamber of untreated or
501 treated cells were collected and centrifugated. Pellets were resuspended in 200 μl and serial

502 dilutions were cultured on agar plates.

503 *Co-infection and co-culture.* At day-0, either *Streptococcus mitis* or *Moraxella catarrhalis*
504 strains grown on agar plates overnight were resuspended in optiMEM medium and cultured in
505 optiMEM medium for 2 to 3 hours at 37°C. After reaching the exponential growth phase,
506 Calu-3 cells grown for two weeks in AIC were infected with 10µl of bacterial suspension
507 containing 1.10^5 CFU. For the control filters, 10 µl of sterile medium was added on top of
508 cells. At day-1, control and infected filters were infected with 1.10^6 of *N. meningitidis* 2C4.3
509 strain as previously described. At day-2, bacteria were harvested by scratching and cultured
510 on selective medium agar plates. The 2C4.3 strain was selected on vancomycin (20 µg/ml)
511 when co-cultured with *S. mitis* and on polymyxin (15 µg/ml) when co-cultured with *M.*
512 *catarrhalis*. During the assay, the cells were incubated at 37°C in a 5% CO₂ incubator.

513

514 **Immunofluorescence assay**

515 *Fixed cells.* For immunofluorescence assays, Calu-3 cells were grown in AIC and infected for
516 24 hours. The filters were fixed with 4% paraformaldehyde for 1 hour at room temperature,
517 washed two times with PBS and permeabilized for 10 minutes with PBS-0.1% X-100 Triton
518 and 10 minutes in PBS-0.1%BSA 0,1% X-100 Triton (staining buffer). The cells were then
519 incubated with an anti-*N. meningitidis* strain 2C4.3 (anti 2C4.3) (and an anti-MUC5AC
520 monoclonal antibody (clone 45M1; life technologies) in staining buffer for 2 hours. After
521 three washes in PBS, the filters were incubated with Alexa-conjugated secondary antibodies
522 for 2 hours. Nuclei DNA and actin were respectively stained with DAPI at 1 µg/mL and
523 Alexa-conjugated phalloidin (Invitrogen). After several washes, the membranes were cut from
524 the plastic support and the coverslips were mounted in Mowiol for observation.

525 *Living cells.* Because the mucus could not be easily preserved through fixation, its production
526 over time was monitored by imaging living cells labeled with an Alexa-conjugated Dextran at

527 1 mg/ml (MW 10000, Life technologies) and Cell Trace Calcein Red Orange AM at 2.5 μ M
528 (Life technologies) was used to stain the epithelium. The cell tracer was added in the basal
529 chamber for one hour while the dextran solution was added on top of cells. Both solutions
530 were removed and washed before confocal acquisition. During acquisition, the cells were
531 maintained at 37°C under 5% CO₂.

532

533 **Image analysis**

534 For three-dimensional reconstruction, image acquisition was performed on a laser-scanning
535 confocal microscope (Leica TCS SP5). Fluorescence microscopy images were collected and
536 processed using the Leica Application Suite AF Lite software. Each channel was adjusted for
537 better visualization. 3D reconstruction, z-stack pictures and post-treatment analyses were
538 performed using Imaris software.

539

540 **Electron microscopy**

541 *Chemicals.* Crystalline osmium tetroxide (OsO₄), sodium cacodylate, 25% glutaraldehyde
542 and Epon were from Euromedex (Souffelweyersheim, France). Hexamethyldisilazane
543 (HMDS) was from Sigma-Aldrich (Lyon, France). Perfluoro-compound FC-72 was from
544 Fisher Scientific (Illkirch, France).

545 *Electron microscopy.* All incubations were performed at room temperature. Whole inserts
546 were fixed in 1% OsO₄ diluted in FC-72 for 90 minutes, rinsed in FC-72 for 30 min and fixed
547 in 2.5% glutaraldehyde diluted in 0.1 M sodium cacodylate buffer, pH 7.4 for 90 minutes. The
548 inserts were then rinsed in cacodylate buffer (2x30 minutes) and immersed in an ascending
549 concentration of ethanol solutions (30%, 50%, 70%, 95%, 100%, 100%, 100% - 10 minutes
550 each) for dehydration. For SEM, dehydration was completed with HMDS/ethanol (1/1, v/v)
551 for 10 minutes and HMDS for 10 minutes. After overnight air drying, each filter was removed

552 from the insert using a small scalpel blade, placed on a double-sided sticky tape on the top of
553 an aluminum stub and sputter coated with Au/Pd. Images were acquired using a Jeol LV6510
554 (Jeol, Croissy-sur-Seine, France). For TEM, inclusion was performed by immersing the
555 inserts in a Epon/ethanol mixture of increasing Epon concentration (1/3 for 60 minutes, 1/1
556 for 60 minutes, 3/1 overnight) and finally in pure Epon (two changes in 48 hours). Each filter
557 was removed from the insert and placed in an embedding capsule, with cells facing down.
558 After resin polymerisation (2h at 37°C then 72h at 60°C), the block was sectioned so as to
559 produce section of the cell layer. Ultrathin sections (80 nm) were stained in lead citrate and
560 examined in a Jeol 100S (Jeol, Croissy-sur-Seine, France) at an accelerating voltage of 80 kV.
561 Living bacteria were defined as circular cells and electron dense.

562

563 **Desiccation assay**

564 Plastic wells were coated with optiMEM as a control or with mucus overnight. The mucus
565 was extracted from Calu-3 cultured in AIC for two weeks using 0.2% β-mercaptoethanol in
566 optiMEM (3 washes of 20 minutes each). For infection, $5 \cdot 10^6$ bacteria in 100 μl of media
567 were added on top of the coated plastic well and incubated at 37°C under 5% CO₂ overnight.
568 The next day, culture supernatants were gently removed and sedimented bacteria were
569 exposed to desiccation for 0, 30, 60 and 120 minutes. Bacteria were harvested and enumerated
570 by quantitative culture into agar plates.

571

572 **Quantitative RT-PCR**

573 *RNA isolation:* Total RNA was isolated from *N. meningitidis* cultured at 37°C in optiMEM
574 medium for 3 hours (exponential growth phase), overnight (stationary phase), or from
575 infected cells (AIC) after 24 hours. In those three conditions, bacteria were pelleted by
576 centrifugation at max speed in a microcentrifuge for 2 minutes and quickly resuspended in

577 cold Trizol solution.

578 Samples were frozen and stored at -80°C. Samples were then treated with chloroform and the
579 aqueous phase was collected and used in the RNeasy Clean-up protocol (Qiagen). RNA
580 samples were incubated with turbo DNase (Invitrogen) for 1 hour at 37°C before cleaning-up
581 on RNeasy mini-column. Elution of RNA was done in nuclease-free water and 1 µl of
582 rRNasin (Promega) was added before storage.

583 *Retrotranscription:* cDNA synthesis reactions were carried out using the Lunascript RT
584 Supermix kit (NEB) and 500 ng of RNA was used for each reaction.

585 Quantitative RT-PCR: The 20 µl reaction consisted of 10 µl Luna Universal qPCR Master
586 Mix, 0.5 µl 10 µM of each primer, 1 µl of cDNA and 8 µl of nuclease-free water. Pairs of
587 primers were designed with Primer3Plus software (*pilE* forward
588 TTTGCGACTGTAACGCTTTG, reverse GCCATCCTTTTGGCTGAAGG ; *porA* forward
589 TCCCTTGAAAAACCATCAGG, reverse CAATTCGGTCGTACTGTTT ; *nadA* forward
590 AAATTAGAAGCCGTGGCTGA, reverse TGCAGCGACAGCTTCGGCCT ; *fhbp* forward
591 CATAACGCCTTCAACCAACT, reverse GTTCGGCGGCGGCAAGCTCG, *nhbA* forward
592 AAACGCCATTAGCCACATTC, reverse CCACGGCACCGAATATGCCA; *pgm* forward
593 GCGAAGCCATAATGGAAAAA, reverse CTTTGCGGCAGGTTGTTTAA) *TonB* forward
594 TCAGCAGCCTAAGGAAGAGC, reverse CTGCCTTCTCCGCGCCCGT ; *LbpA* forward
595 GATAAGGCGGTGTTGTCGTT, reverse TGGAAGCATCGTAACCGAAG ; *TbpA* forward
596 GCAGTGGGGGATTCAGAGTA, reverse GGATGGGTATCCTCAACCGG ; *FetA* forward
597 CGGCAGAAAATAATGCCAAT, reverse GTGCCGTTGCCGCCGCGAA ; *ctrA* forward
598 GTTTGGCGATGGTTATGCTT, reverse CGGCCTTTAATAATTTCTG; *mtrC* forward
599 CCGTACCGAACGATCAGAAT, reverse CTTCAGACCCGACGTAACAA ; *OpaB* forward
600 CTTGTCCGCCATTTACGATT, reverse TGATACAAGCTTGCCTGGCT ; *OpaC* forward
601 AACATCCGTACGCATTCCAT, reverse AAGCCGAGCGAGGAGACGGC. Gene

602 expression levels were normalized by that of the housekeeping gene *pgm* (NMV_1606).

603 Appropriate no-RT controls were carried out to ensure accuracy of the results.

604

605 Cytokine quantification assay

606 *Sample preparations:* Calu-3 cells were grown on transwell either in AIC or LCC during two

607 weeks. For AIC, cells were incubated at 37°C for 20 minutes with 100 µl of Ringer solution

608 and that apical supernatants were collected. This step was repeated once, and samples were

609 kept on ice. For liquid interfaced culture, the 100 µl of medium in the apical chamber was

610 collected and cells were washed with another volume of 100µl of optiMEM medium. All

611 samples were vortexed and centrifugated at 4°C for 5 minutes at maximum speed to eliminate

612 bacteria and debris. Supernatants were harvested, snap-freeze in liquid nitrogen and kept at -

613 80°C before processing.

614 *Cytokines measurement:* cytokines in cell supernatants were quantified by

615 electrochemiluminescence multiplex assay kits from Meso Scale Discovery (Rockville, MD,

616 USA). Briefly, 25 µl of supernatant were added to 96-well multi-spot plates and the assays

617 were performed following the manufacturer's instructions. Plates were read on the

618 multiplexing imager Sector S600 (Meso Scale Discovery). All samples were measured in

619 duplicate.

620

621 **Mucin glycosylation analysis**

622 *Isolation and purification of mucins secreted by Calu-3 cells.* Cells were solubilized in 4 M

623 guanidine chloride reduction buffer containing 10 mM DTT, 5 mM

624 ethylenediaminetetraacetic acid, 10 mM benzamidine, 5 mM *N*-ethylmaleimide, 0.1 mg/ml

625 soy bean trypsin inhibitor and 1 mM phenylmethanesulfonyl fluoride. Two ml of reduction

626 buffer was added to each apical chamber and incubated overnight at room temperature. Cell

627 suspensions were then gently agitated by pipetting and each of the 5 filter suspensions per
628 condition were pooled in a single aliquot. CsCl was added to an initial density of 1.4 g/ml and
629 mucins were purified by isopycnic density-gradient centrifugation (Beckman Coulter LE80 K
630 ultracentrifuge; 70.1 Ti rotor, 417,600 g at 15°C for 72 hours). Fractions of 1 ml were
631 collected from the bottom of the tube and analysed for periodic acid-Schiff (PAS) reactivity
632 and density. The mucin-containing fractions were pooled, dialyzed against water and
633 lyophilized.

634 *Release of oligosaccharides from mucin by alkaline borohydride treatment.* Mucins were
635 submitted to β -elimination under reductive conditions (0.1 M KOH, 1 M KBH₄ for 24 hours
636 at 45°C) and the mixture of oligosaccharide alditols was dried on a rotavapor (Buchi) at 45°C.
637 Borate salts were eliminated by several co-evaporations with methanol before purification by
638 cation exchange chromatography (Dowex 50x2, 200-400 mesh, H + form).

639 *Permethylation and mucin glycosylation analysis by MALDI TOF MS.* Permethylation of the
640 mixture of oligosaccharide alditols was carried out with the sodium hydroxide procedure
641 described by Ciucanu and Kerek (1984) [45]. After derivatization, the reaction products were
642 dissolved in 200 μ l of methanol and further purified on a C18 Sep-Pak column (Waters,
643 Milford, MA). Permethylated oligosaccharides were analyzed by MALDI TOF MS in a
644 positive ion reflective mode as [M+Na]⁺. Quantification through the relative percentage of
645 each oligosaccharide was calculated based on the integration of peaks on MS spectra.

646

647 **Statistics**

648 Statistical analyses were performed using GraphPad Prism 8 Software. One-way analysis of
649 variance (ANOVA) or Student *t* test were used in this study. P-values of $p < 0.05$ were
650 considered to indicate statistical significance. Each images presented in this work were
651 representative images.

652 **ACKNOWLEDGEMENTS**

653 We thank Nicolas Goudin of the Necker Institute imaging facility for his technical support.

654 We thank Emmanuelle Bille for her careful reading of the manuscript. We thank Karine

655 Bailly of the Cochin Institute Cytometry and Immunobiology facility (CYBIO) for her

656 excellent technical assistance. This work was supported by ANR-15-CE15-0002-01 grants.

657 XN and MC are also supported by INSERM, CNRS, Université de Paris and the Fondation

658 pour la Recherche Médicale. CRM was supported by the Research Federation FRABio (Univ.

659 Lille, CNRS, FR 3688, FRABio, Biochimie Structurale et Fonctionnelle des Assemblages

660 Biomoléculaires), the CNRS (Unité mixte de Recherche CNRS/ULille 8576) and the

661 Ministère de l'Enseignement Supérieur et de la Recherche.

662

663

664

665

666

667

668

669

670

671

672

673






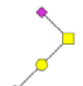

674

675

676

677 **Table 1. Highlights on sialylated oligosaccharides, and their non sialylated form,**
 678 **identified on Calu-3 mucins, before (control) and after infection with *N. meningitidis***
 679 **(*Nm*) or co-infection with *N. meningitidis* and *S. mitis* (*Nm+Sm*).** The relative percentage of
 680 each oligosaccharide was calculated based on the integration of peaks on MS spectra. Two
 681 independent experiments of 5 different filters were studied in bulk. Results are presented as
 682 the mean relative percentage of each oligosaccharide \pm SEM.

683

Proposed structures or sequences of oligosaccharides	[M+Na] ⁺	Calu-3 control	Calu-3 <i>Nm</i>	Calu-3 <i>Nm+Sm</i>
	534	53.2 \pm 1.2	34.4 \pm 1.6	86.7 \pm 8.8
	575	1.3 \pm 1.2	0	0.3 \pm 0.3
	895	29.8 \pm 3.1	41.7 \pm 0.4	3 \pm 3
	983	3.1 \pm 1.1	3.7 \pm 0.4	6.4 \pm 2.9
	1071	0.3 \pm 0.1	0.2 \pm 0.2	0.8 \pm 0.8
	1256	3.6 \pm 1.6	13.4 \pm 1.2	0
	1344	1.2 \pm 0.5	4.2 \pm 0.4	0
2 Hex, 1 HexNAc, 2 NeuAc, GalNAcol	1705	1.3 \pm 1.3	0.6 \pm 0.1	0
3 Hex, 2 HexNAc, 1 NeuAc, GalNAcol	1793	0.3 \pm 0.3	0.1 \pm 0.1	0

684

685

686

687

688

689 **LEGENDS**

690

691 **Figure 1: *N. meningitidis* proliferation in an Air Interfaced Culture model.** (A) Confocal
692 3D reconstructions showing *N. meningitidis* proliferation, 24 hours after infection of Calu-3
693 cells. Meningococci were labeled with anti-2C43 antibody (green). Cells were stained with
694 Alexa-conjugated Phalloïdin (red). Nuclei were stained with dapi (blue). Upper panel: 3D
695 view; Lower panel: Apical view. Bar: 20 μm . (B) Number of CFU of *N. meningitidis* per well
696 24 hours after infection (10^6 bacteria). Data were expressed as mean CFU per filter \pm SEM
697 (statistical significance: * $p < 0.05$, ** $p < 0.01$; One-way ANOVA; At least five filters; three
698 independent experiments). (C) Desiccation assay. Plates were coated with the mucus obtained
699 from Calu-3 cells or with the culture media as control. Bacteria were then grown overnight in
700 these wells containing culture media. The media was then gently removed. Bacteria were
701 dried for 0, 30, 60 or 120 minutes. The number of CFU was then assessed. Data were
702 expressed as mean of CFU per ml \pm SEM (statistical significance: ** $p < 0.01$; Student *t* test;
703 At least four wells; two independent experiments).

704

705 **Figure 2: *N. meningitidis* colonize the outer mucus.** Calu-3 cells grown in AIC were
706 infected for 24 hours with 10^6 bacteria. (A) After infection, the outer layer of the mucus (outer
707 mucus) was dissociated from the cell-attached mucus using N-acetylcysteine. Bacterial load
708 in the N-acetylcysteine fraction or the cell-attached fraction was determined. Data were
709 expressed as mean percentage of CFU \pm SEM (At least five filters; three independent
710 experiments). (B) Scanning electron microscopy images showing bacteria trapped in the
711 mucus. *: bacteria; arrow: bacteria that directly interact with Calu-3 cells. Bar: 10 μm . (C)
712 Transmission electron microscopy images showing bacteria in the mucus (left) or in contact
713 with cells (right). *: dying bacteria; arrow: bacteria adherent to Calu-3 cells. Bar: 2 μm . (D)

714 Z-stack from confocal 3D reconstruction of two different Calu-3 cell layers infected with *N.*
715 *meningitidis*. Calu-3 cell layers were fixed and immuno-stained with anti-2C4.3 antibody
716 (green) and anti-MUC5AC antibody (purple). Cells were stained with A546-phalloidin (red)
717 and nuclei were stained with dapi (blue). Bar: 20 μm .

718

719 **Figure 3: *N. meningitidis* do not cross the epithelial layer.** (A) Z-stack from confocal 3D
720 reconstruction of Calu-3 cell layer infected 24 hours with 10^6 bacteria of the wild type strain
721 (2C4.3 WT) or the strain defective for type IV pili (2C4.3 $\Delta pilE$). Calu-3 cell layer were fixed
722 and immuno-stained with anti-2C4.3 antibody (green). Cells were stained with Alexa-
723 conjugated phalloidin (red) and nuclei were stained with dapi (blue). Bar: 20 μm . (B)
724 Transmission electron microscopy images (longitudinal sections) of Calu-3 cell layer infected
725 for 24 hours with 10^6 wild type meningococci. Bar: 2 μm . (C) Kaplan-Meier plot showing the
726 traversal of wild type *N. meningitidis* across the Calu-3 cell layer. Data were expressed as
727 percentage of invaded basal chamber (untreated cells: 8 filters infected with 10^4 or 10^2
728 bacteria, three independent experiments; IL-4/13 treated cells: 4 filters infected with 10^4 or
729 10^2 bacteria, two independent experiments).

730

731 **Figure 4: Expression of virulence factors.** Total RNA obtained from a 3 hours or 24 hours
732 broth culture or harvested following 24 hours of infection of Calu-3 cells using AIC, was
733 prepared. Gene expression of *pilE*, *opaB*, *opaC*, *tbpA*, *lbpA*, *fetA*, *tonB*, *mtrC*, *porA*, *nadA*,
734 *fHbp*, *nhbA* and *ctrA* was analyzed by quantitative RT-PCR. Gene expression was normalized
735 to that of *pgm* and expressed as relative expression \pm SEM (statistical significance: ****
736 $p < 0.0001$; ** $p < 0.01$; * $p < 0.05$; ns: no significant difference; One-way ANOVA; two
737 independent experiment in triplicate).

738

739 **Figure 5: Cytokine expression by infected Calu-3 cells grown in AIC and LCC.** Cytokine
740 secretion was investigated in the mucus of non-infected and infected in AIC for 24 hours or in
741 the supernatant of non-infected and infected Calu-3 cells, in LCC for 24 hours. Data were
742 expressed as mean \pm SEM of fold increase between infected and non-infected conditions
743 (statistical significance: **** $p < 0.0001$, *** $p < 0.001$, ** $p < 0.01$, * $p < 0.05$; One-way
744 ANOVA: at least two filters read in duplicate).

745

746 **Figure 6: Co-infection with *S. mitis* and *M. catarrhalis*.** (A) Schematic representation of the
747 protocol followed for co-infection. (B) At day 1, cells were infected with 10^5 bacteria (*S. mitis*
748 or *M. catarrhalis*). At day 2, cells were then infected with 10^6 meningococci. At day 3,
749 bacteria were collected and CFU were determined. CFU of meningococci after 24 hours of
750 co-culture were expressed as mean percentage of the control experiment \pm SEM (CFU of
751 meningococci in mono-culture) (statistical significance: ** $p < 0.01$, * $p < 0.05$; Student *t* test;
752 At least five filters, three independent experiments).

753

754 **Supplementary figure 1: Calu-3 cells grown using AIC.** (A) Confocal 3D reconstructions
755 of living Calu-3 cells showing accumulation of the mucus after two weeks of culture in AIC.
756 The mucus was labeled with Alexa-conjugated Dextran (cyan) and cells were stained with
757 Cell Trace Calcein Red Orange, AM (red). Bar: 20 μ m. (B) Transmission electron microscopy
758 images (transversal section). *: Tight junction; arrow: mucin-containing vesicles; μ V:
759 microvilli. M: mucus. Bar: 2 μ m.

760

761 **Supplementary figure 2: Dying and living *N. meningitidis*.** Transmission electron
762 microscopy images (longitudinal section) showing dying and living bacteria inside the mucus
763 (A) and dying bacteria inside a cell (B). DB: Dead bacteria; LB: living bacteria. Bar: 1 μ m.

764

765 **Supplementary figure 3: Culture of Calu-3 cells in the presence of IL-4 and IL-13; and**

766 **infection of Calu-3 cells. (A)** Measurement of the TEER of Calu-3 cell layer cultured in AIC

767 using 0.4 μ m pore membrane or 3 μ m pore membrane, with or without addition of 5 ng/ml IL-

768 4 or IL-13 for 24 hours. TEER were expressed as mean Ohm.cm² \pm SEM (statistical

769 significance: *** p<0.001, ** p<0.01; One way-ANOVA; 0.4 Vs 3 μ m pore membrane: three

770 filters; Control Vs IL-4/13: 4 filters, two independent experiments). **(B)** Count of

771 meningococci 24 hours after infection of Calu-3 cells, grown in AIC, with 10² or 10⁴ or 10⁶

772 bacteria. Data were expressed as mean of CFU per filter \pm SEM. Six filters, two independent

773 experiments. **(C)** Confocal 3D reconstructions showing *N. meningitidis* proliferation. Twenty-

774 four hours after infection of Calu-3 cells with 10² or 10⁴ or 10⁶ bacteria, cells were fixed and

775 immuno-stained with anti-2C4.3 antibody (green). Cells were stained using Alexa-conjugated

776 phalloidin (in red). Nuclei were stained with dapi (blue). Bar: 20 μ m.

777

778 **Supplementary figure 4: Co-culture of *N. meningitidis* with *S. mitis* in broth.** BHI broth

779 co-cultures were performed during 24 hours and *N. meningitidis* CFU determined. The

780 number of meningococci after 24 hours of co-culture was expressed as mean percentage of

781 the control experiment \pm SEM (control: CFU of meningococci in mono-culture) (statistical

782 significance: **** p<0.0001, * p<0.01; Student *t* test; Four wells, two independent

783 experiments).

784

785

786

787

788

789 **REFERENCES**

790

- 791 1 Join-Lambert, O. *et al.* Meningococcal interaction to microvasculature triggers the tissular
792 lesions of purpura fulminans. *The Journal of infectious diseases* **208**, 1590-1597,
793 doi:10.1093/infdis/jit301 (2013).
- 794 2 Brandtzaeg, P. & van Deuren, M. Classification and pathogenesis of meningococcal
795 infections. *Methods Mol Biol* **799**, 21-35, doi:10.1007/978-1-61779-346-2_2 (2012).
- 796 3 Lecuyer, H., Borgel, D., Nassif, X. & Coureuil, M. Pathogenesis of meningococcal purpura
797 fulminans. *Pathogens and disease* **75**, doi:10.1093/femspd/ftx027 (2017).
- 798 4 Capel, E. *et al.* Peripheral blood vessels are a niche for blood-borne meningococci. *Virulence*
799 **8**, 1808-1819, doi:10.1080/21505594.2017.1391446 (2017).
- 800 5 Lecuyer, H. *et al.* An ADAM-10 dependent EPCR shedding links meningococcal interaction
801 with endothelial cells to purpura fulminans. *PLoS pathogens* **14**, e1006981,
802 doi:10.1371/journal.ppat.1006981 (2018).
- 803 6 Bonazzi, D. *et al.* Intermittent Pili-Mediated Forces Fluidize Neisseria meningitidis Aggregates
804 Promoting Vascular Colonization. *Cell* **174**, 143-155 e116, doi:10.1016/j.cell.2018.04.010
805 (2018).
- 806 7 Simonis, A. & Schubert-Unkmeir, A. Interactions of meningococcal virulence factors with
807 endothelial cells at the human blood-cerebrospinal fluid barrier and their role in
808 pathogenicity. *FEBS letters* **590**, 3854-3867, doi:10.1002/1873-3468.12344 (2016).
- 809 8 Coureuil, M., Lecuyer, H., Bourdoulous, S. & Nassif, X. A journey into the brain: insight into
810 how bacterial pathogens cross blood-brain barriers. *Nature reviews. Microbiology* **15**, 149-
811 159, doi:10.1038/nrmicro.2016.178 (2017).
- 812 9 Cremers, A. J. *et al.* The adult nasopharyngeal microbiome as a determinant of
813 pneumococcal acquisition. *Microbiome* **2**, 44, doi:10.1186/2049-2618-2-44 (2014).
- 814 10 Wang, H. *et al.* Microbiota Composition in Upper Respiratory Tracts of Healthy Children in
815 Shenzhen, China, Differed with Respiratory Sites and Ages. *BioMed research international*
816 **2018**, 6515670, doi:10.1155/2018/6515670 (2018).
- 817 11 Esposito, S. & Principi, N. Impact of nasopharyngeal microbiota on the development of
818 respiratory tract diseases. *Eur J Clin Microbiol Infect Dis* **37**, 1-7, doi:10.1007/s10096-017-
819 3076-7 (2018).
- 820 12 Biesbroek, G. *et al.* Early respiratory microbiota composition determines bacterial succession
821 patterns and respiratory health in children. *American journal of respiratory and critical care*
822 *medicine* **190**, 1283-1292, doi:10.1164/rccm.201407-1240OC (2014).
- 823 13 Santee, C. A. *et al.* Nasopharyngeal microbiota composition of children is related to the
824 frequency of upper respiratory infection and acute sinusitis. *Microbiome* **4**, 34,
825 doi:10.1186/s40168-016-0179-9 (2016).
- 826 14 Ali, M. Y. Histology of the human nasopharyngeal mucosa. *Journal of anatomy* **99**, 657-672
827 (1965).
- 828 15 Freeman, S. C. & Kahwaji, C. I. in *StatPearls* (2018).
- 829 16 Fahy, J. V. & Dickey, B. F. Airway mucus function and dysfunction. *The New England journal*
830 *of medicine* **363**, 2233-2247, doi:10.1056/NEJMra0910061 (2010).
- 831 17 Lillehoj, E. P., Kato, K., Lu, W. & Kim, K. C. Cellular and molecular biology of airway mucins.
832 *International review of cell and molecular biology* **303**, 139-202, doi:10.1016/B978-0-12-
833 407697-6.00004-0 (2013).
- 834 18 Hoegger, M. J. *et al.* Assessing mucociliary transport of single particles in vivo shows variable
835 speed and preference for the ventral trachea in newborn pigs. *Proceedings of the National*
836 *Academy of Sciences of the United States of America* **111**, 2355-2360,
837 doi:10.1073/pnas.1323633111 (2014).

- 838 19 Ganz, T. Antimicrobial polypeptides in host defense of the respiratory tract. *The Journal of*
839 *clinical investigation* **109**, 693-697, doi:10.1172/JCI15218 (2002).
- 840 20 Cole, A. M., Dewan, P. & Ganz, T. Innate antimicrobial activity of nasal secretions. *Infection*
841 *and immunity* **67**, 3267-3275 (1999).
- 842 21 Brandtzaeg, P. Mucosal immunity: induction, dissemination, and effector functions.
843 *Scandinavian journal of immunology* **70**, 505-515, doi:10.1111/j.1365-3083.2009.02319.x
844 (2009).
- 845 22 Virji, M., Alexandrescu, C., Ferguson, D. J., Saunders, J. R. & Moxon, E. R. Variations in the
846 expression of pili: the effect on adherence of *Neisseria meningitidis* to human epithelial and
847 endothelial cells. *Molecular microbiology* **6**, 1271-1279 (1992).
- 848 23 Rudel, T., van Putten, J. P., Gibbs, C. P., Haas, R. & Meyer, T. F. Interaction of two variable
849 proteins (PIL and PilC) required for pilus-mediated adherence of *Neisseria gonorrhoeae* to
850 human epithelial cells. *Molecular microbiology* **6**, 3439-3450 (1992).
- 851 24 Nassif, X. *et al.* Antigenic variation of pilin regulates adhesion of *Neisseria meningitidis* to
852 human epithelial cells. *Molecular microbiology* **8**, 719-725 (1993).
- 853 25 Marceau, M., Beretti, J. L. & Nassif, X. High adhesiveness of encapsulated *Neisseria*
854 *meningitidis* to epithelial cells is associated with the formation of bundles of pili. *Molecular*
855 *microbiology* **17**, 855-863 (1995).
- 856 26 Merz, A. J., Rifken, D. B., Arvidson, C. G. & So, M. Traversal of a polarized epithelium by
857 pathogenic *Neisseriae*: facilitation by type IV pili and maintenance of epithelial barrier
858 function. *Molecular medicine (Cambridge, Mass)* **2**, 745-754 (1996).
- 859 27 Pujol, C., Eugene, E., de Saint Martin, L. & Nassif, X. Interaction of *Neisseria meningitidis* with
860 a polarized monolayer of epithelial cells. *Infection and immunity* **65**, 4836-4842 (1997).
- 861 28 Edwards, V. L., Wang, L. C., Dawson, V., Stein, D. C. & Song, W. *Neisseria gonorrhoeae*
862 breaches the apical junction of polarized epithelial cells for transmigration by activating
863 EGFR. *Cellular microbiology* **15**, 1042-1057, doi:10.1111/cmi.12099 (2013).
- 864 29 Virji, M., Makepeace, K., Ferguson, D. J., Achtman, M. & Moxon, E. R. Meningococcal Opa
865 and Opc proteins: their role in colonization and invasion of human epithelial and endothelial
866 cells. *Molecular microbiology* **10**, 499-510 (1993).
- 867 30 de Vries, F. P., van Der Ende, A., van Putten, J. P. & Dankert, J. Invasion of primary
868 nasopharyngeal epithelial cells by *Neisseria meningitidis* is controlled by phase variation of
869 multiple surface antigens. *Infection and immunity* **64**, 2998-3006 (1996).
- 870 31 Billker, O., Popp, A., Gray-Owen, S. D. & Meyer, T. F. The structural basis of CEACAM-receptor
871 targeting by neisserial Opa proteins. *Trends in microbiology* **8**, 258-260; discussion 260-251
872 (2000).
- 873 32 Sutherland, T. C., Quattroni, P., Exley, R. M. & Tang, C. M. Transcellular passage of *Neisseria*
874 *meningitidis* across a polarized respiratory epithelium. *Infection and immunity* **78**, 3832-3847
875 (2010).
- 876 33 Barrile, R. *et al.* *Neisseria meningitidis* subverts the polarized organization and intracellular
877 trafficking of host cells to cross the epithelial barrier. *Cellular microbiology*,
878 doi:10.1111/cmi.12439 (2015).
- 879 34 Stephens, D. S., Hoffman, L. H. & McGee, Z. A. Interaction of *Neisseria meningitidis* with
880 human nasopharyngeal mucosa: attachment and entry into columnar epithelial cells. *The*
881 *Journal of infectious diseases* **148**, 369-376 (1983).
- 882 35 Stephens, D. S. *et al.* Analysis of damage to human ciliated nasopharyngeal epithelium by
883 *Neisseria meningitidis*. *Infection and immunity* **51**, 579-585 (1986).
- 884 36 Stephens, D. S. & Farley, M. M. Pathogenic events during infection of the human
885 nasopharynx with *Neisseria meningitidis* and *Haemophilus influenzae*. *Rev Infect Dis* **13**, 22-
886 33 (1991).
- 887 37 Read, R. C. *et al.* Experimental infection of human nasal mucosal explants with *Neisseria*
888 *meningitidis*. *J Med Microbiol* **42**, 353-361 (1995).

- 889 38 Kreft, M. E. *et al.* The characterization of the human cell line Calu-3 under different culture
890 conditions and its use as an optimized in vitro model to investigate bronchial epithelial
891 function. *European journal of pharmaceutical sciences : official journal of the European*
892 *Federation for Pharmaceutical Sciences* **69**, 1-9, doi:10.1016/j.ejps.2014.12.017 (2015).
- 893 39 Stearns, J. C. *et al.* Culture and molecular-based profiles show shifts in bacterial communities
894 of the upper respiratory tract that occur with age. *The ISME journal* **9**, 1246-1259,
895 doi:10.1038/ismej.2014.250 (2015).
- 896 40 Bogaert, D. *et al.* Variability and diversity of nasopharyngeal microbiota in children: a
897 metagenomic analysis. *PloS one* **6**, e17035, doi:10.1371/journal.pone.0017035 (2011).
- 898 41 Teo, S. M. *et al.* The infant nasopharyngeal microbiome impacts severity of lower respiratory
899 infection and risk of asthma development. *Cell host & microbe* **17**, 704-715,
900 doi:10.1016/j.chom.2015.03.008 (2015).
- 901 42 Etienne-Manneville, S. & Hall, A. Integrin-mediated activation of Cdc42 controls cell polarity
902 in migrating astrocytes through PKCzeta. *Cell* **106**, 489-498 (2001).
- 903 43 Merz, A. J., Enns, C. A. & So, M. Type IV pili of pathogenic *Neisseriae* elicit cortical plaque
904 formation in epithelial cells. *Molecular microbiology* **32**, 1316-1332 (1999).
- 905 44 Ahdieh, M., Vandenbos, T. & Youakim, A. Lung epithelial barrier function and wound healing
906 are decreased by IL-4 and IL-13 and enhanced by IFN-gamma. *American journal of physiology*
907 **281**, C2029-2038, doi:10.1152/ajpcell.2001.281.6.C2029 (2001).
- 908 45 Derrien, M. *et al.* Mucin-bacterial interactions in the human oral cavity and digestive tract.
909 *Gut Microbes* **1**, 254-268, doi:10.4161/gmic.1.4.12778 (2010).
- 910 46 Rouabhia, M., Ross, G., Page, N. & Chakir, J. Interleukin-18 and gamma interferon production
911 by oral epithelial cells in response to exposure to *Candida albicans* or lipopolysaccharide
912 stimulation. *Infection and immunity* **70**, 7073-7080, doi:10.1128/iai.70.12.7073-7080.2002
913 (2002).
- 914 47 Hadifar, S. *et al.* Comparative study of interruption of signaling pathways in lung epithelial
915 cell by two different *Mycobacterium tuberculosis* lineages. *Journal of cellular physiology* **234**,
916 4739-4753, doi:10.1002/jcp.27271 (2019).
- 917 48 Oyanagi, T. *et al.* Suppression of MUC5AC expression in human bronchial epithelial cells by
918 interferon-gamma. *Allergology international : official journal of the Japanese Society of*
919 *Allergology* **66**, 75-82, doi:10.1016/j.alit.2016.05.005 (2017).
- 920 49 Zhu, Y., Song, D., Song, Y. & Wang, X. Interferon gamma induces inflammatory responses
921 through the interaction of CEACAM1 and PI3K in airway epithelial cells. *Journal of*
922 *translational medicine* **17**, 147, doi:10.1186/s12967-019-1894-3 (2019).
- 923 50 McNeil, L. K. *et al.* Role of factor H binding protein in *Neisseria meningitidis* virulence and its
924 potential as a vaccine candidate to broadly protect against meningococcal disease.
925 *Microbiology and molecular biology reviews : MMBR* **77**, 234-252,
926 doi:10.1128/MMBR.00056-12 (2013).
- 927 51 Peters-Hall, J. R. *et al.* Quantitative proteomics reveals an altered cystic fibrosis in vitro
928 bronchial epithelial secretome. *American journal of respiratory cell and molecular biology* **53**,
929 22-32, doi:10.1165/rcmb.2014-0256RC (2015).
- 930 52 Kulkarni, H. S., Liszewski, M. K., Brody, S. L. & Atkinson, J. P. The complement system in the
931 airway epithelium: An overlooked host defense mechanism and therapeutic target? *The*
932 *Journal of allergy and clinical immunology* **141**, 1582-1586 e1581,
933 doi:10.1016/j.jaci.2017.11.046 (2018).
- 934 53 Pericone, C. D., Overweg, K., Hermans, P. W. & Weiser, J. N. Inhibitory and bactericidal
935 effects of hydrogen peroxide production by *Streptococcus pneumoniae* on other inhabitants
936 of the upper respiratory tract. *Infection and immunity* **68**, 3990-3997,
937 doi:10.1128/iai.68.7.3990-3997.2000 (2000).
- 938 54 Okahashi, N. *et al.* Hydrogen peroxide contributes to the epithelial cell death induced by the
939 oral mitis group of streptococci. *PloS one* **9**, e88136, doi:10.1371/journal.pone.0088136
940 (2014).

FIGURE 1

bioRxiv preprint doi: <https://doi.org/10.1101/690610>; this version posted July 2, 2019. The copyright holder for this preprint (which was not certified by peer review) is the author/funder. All rights reserved. No reuse allowed without permission.

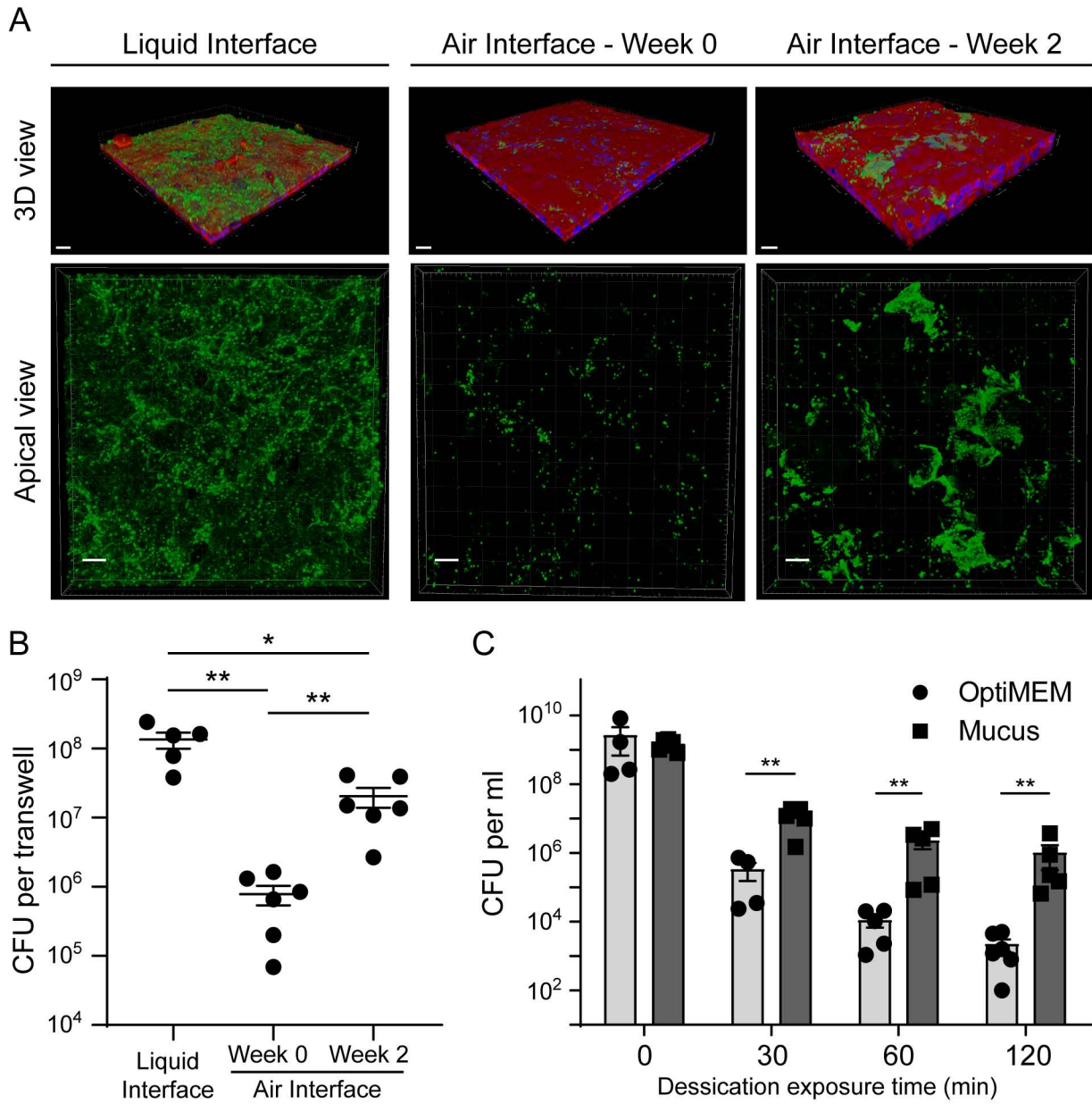


FIGURE 2

bioRxiv preprint doi: <https://doi.org/10.1101/690610>; this version posted July 2, 2019. The copyright holder for this preprint (which was not certified by peer review) is the author/funder. All rights reserved. No reuse allowed without permission.

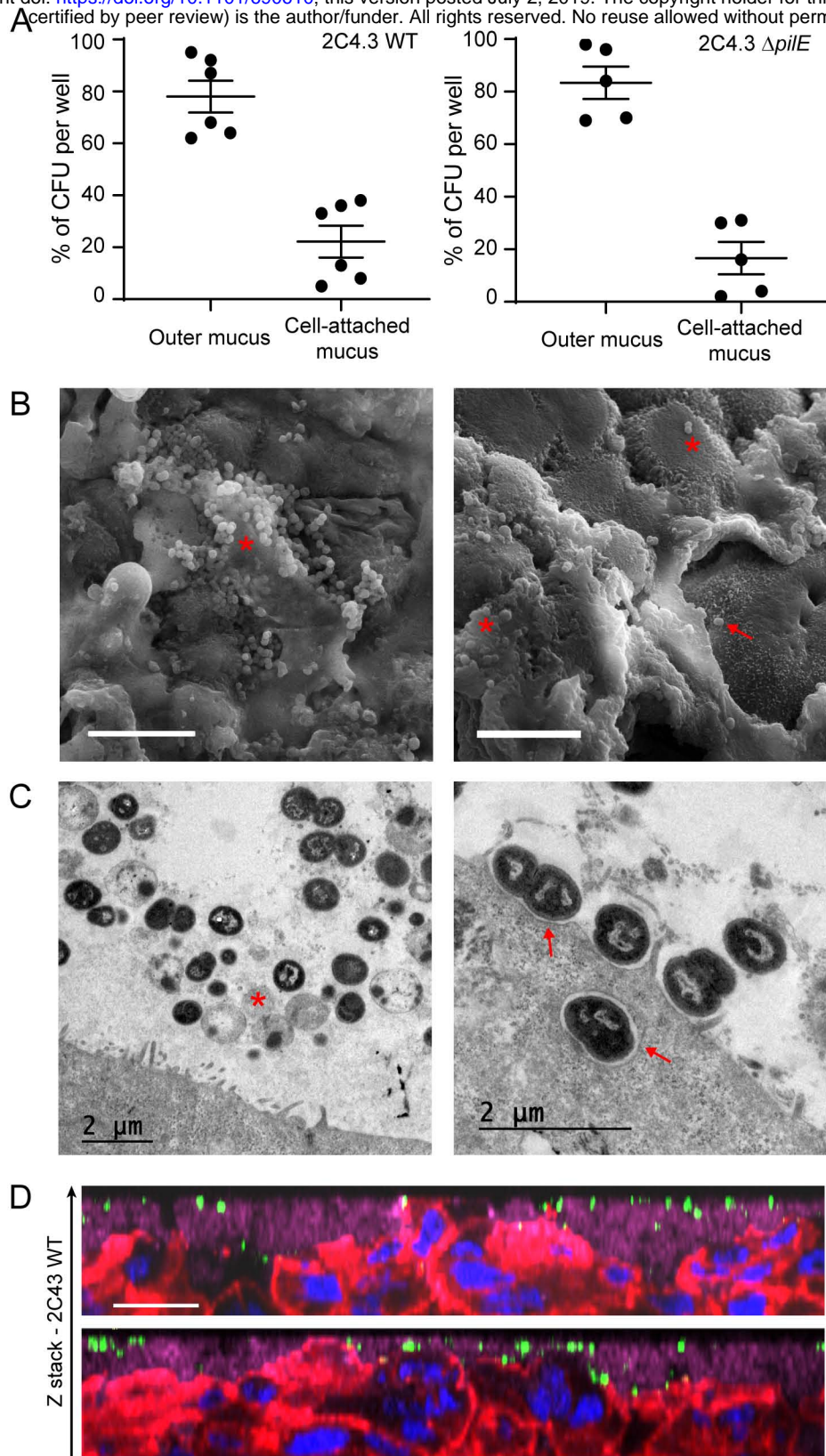


FIGURE 3

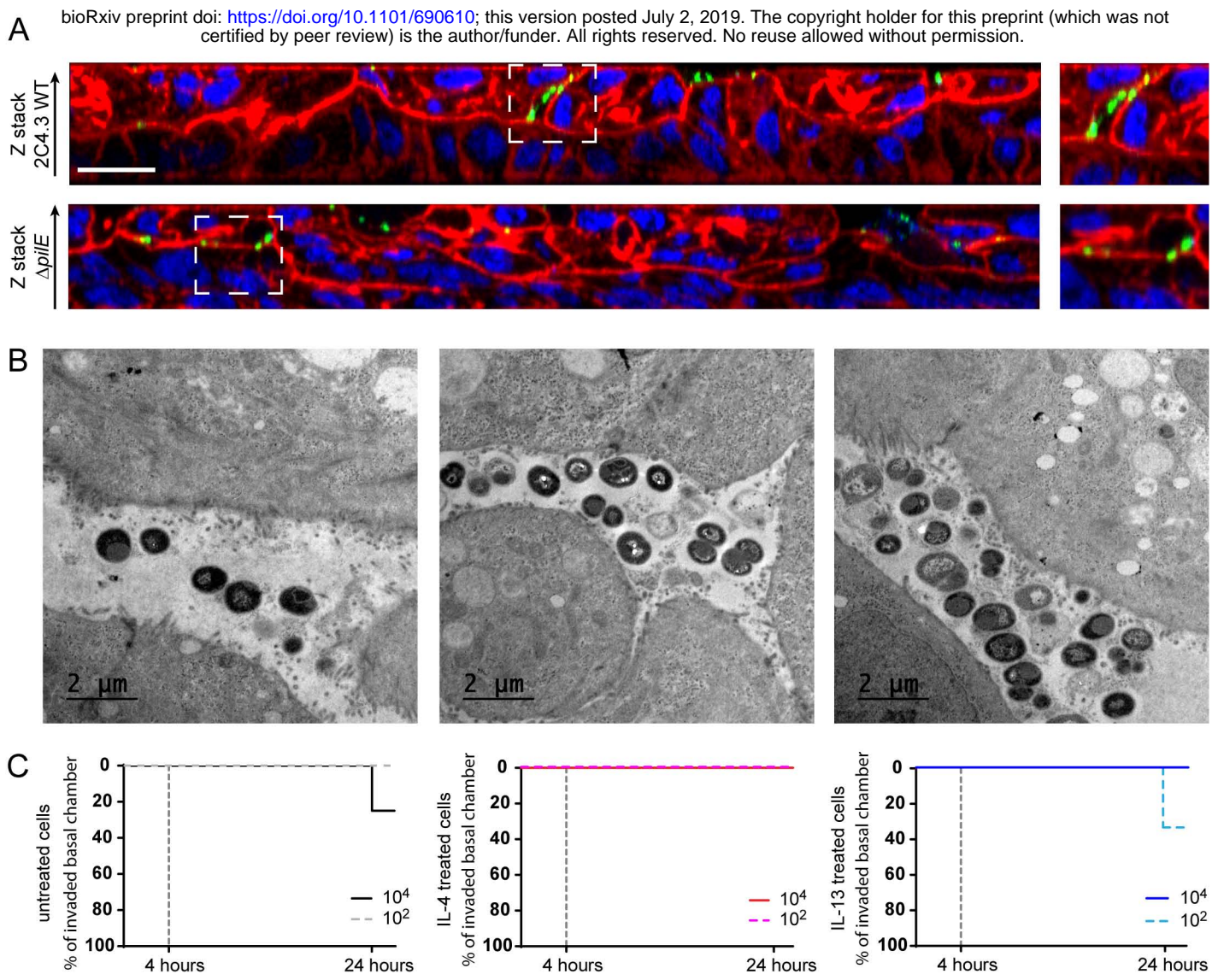


FIGURE 4

bioRxiv preprint doi: <https://doi.org/10.1101/690610>; this version posted July 2, 2019. The copyright holder for this preprint (which was not certified by peer review) is the author/funder. All rights reserved. No reuse allowed without permission.

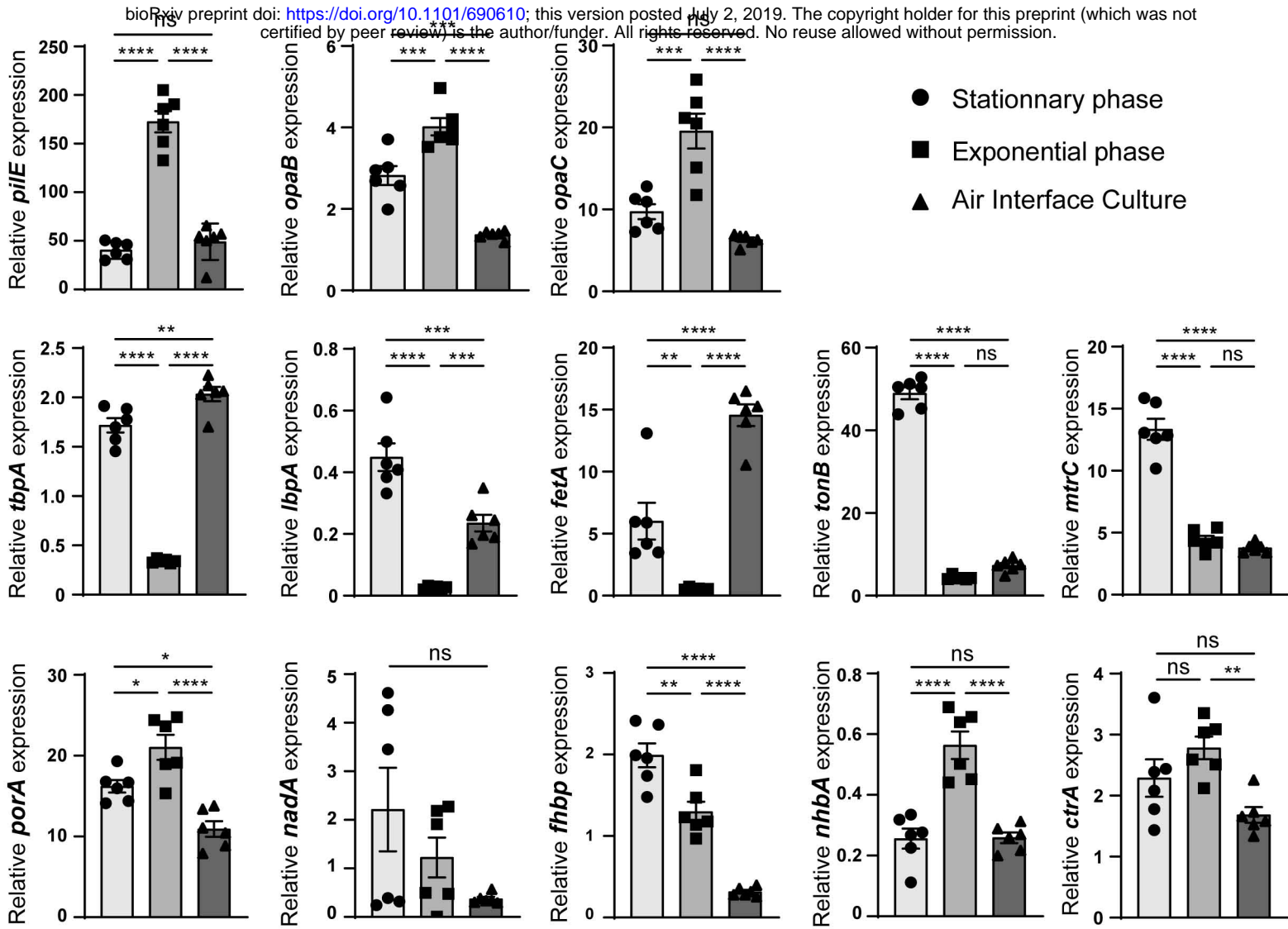


FIGURE 5

bioRxiv preprint doi: <https://doi.org/10.1101/690610>; this version posted July 2, 2019. The copyright holder for this preprint (which was not certified by peer review) is the author/funder. All rights reserved. No reuse allowed without permission.

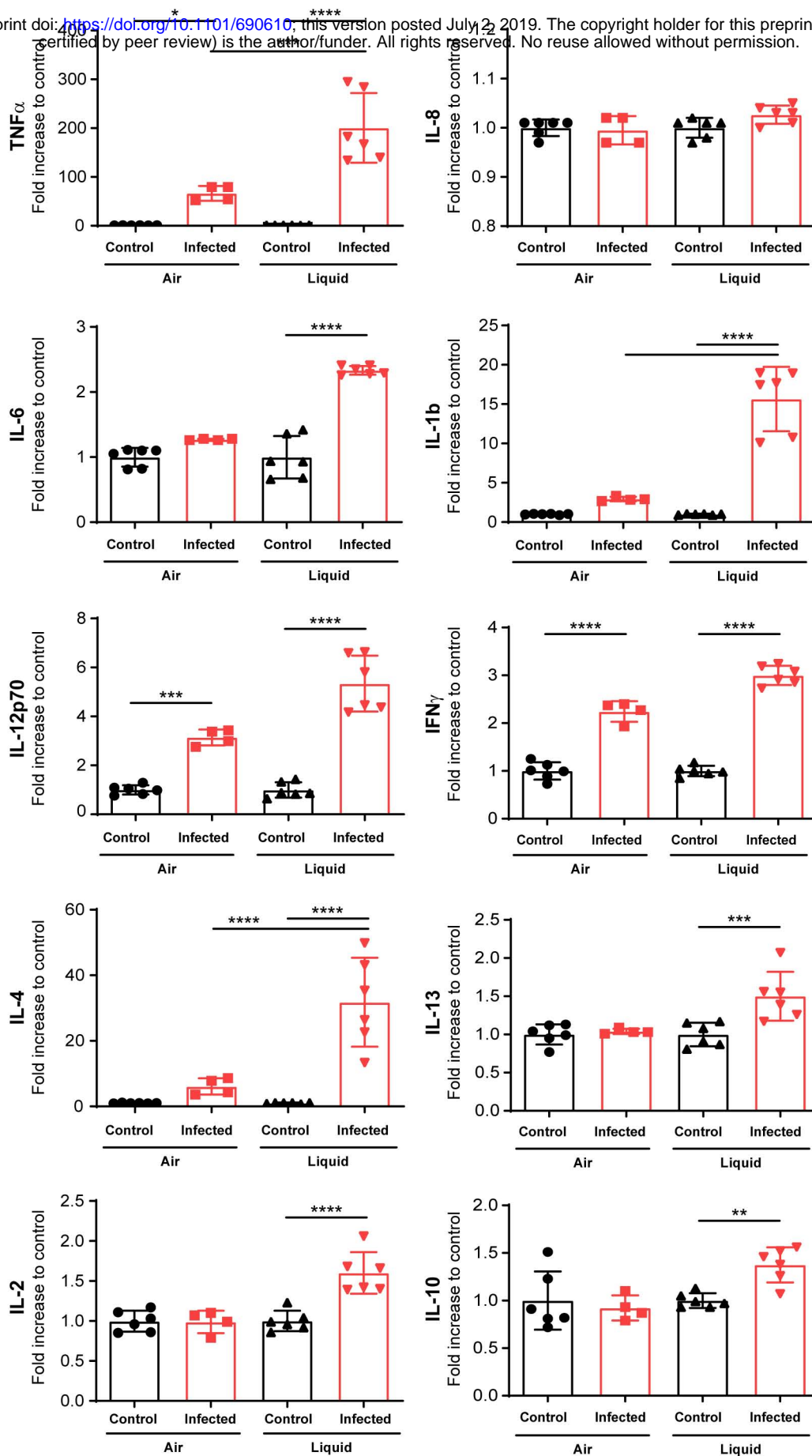


FIGURE 6

bioRxiv preprint doi: <https://doi.org/10.1101/690610>; this version posted July 2, 2019. The copyright holder for this preprint (which was not certified by peer review) is the author/funder. All rights reserved. No reuse allowed without permission.

